X-ray and Quasi-Elastic Light-Scattering Studies of Sodium Deoxycholate

ARTICLE *in* LANGMUIR · JULY 1998

Impact Factor: 4.46 · DOI: 10.1021/la971312r

X-ray and Quasi-Elastic Light-Scattering Studies of Sodium Deoxycholate

A. A. D'Archivio,† L. Galantini,† E. Giglio,*,‡ and A. Jover§

Dipartimento di Chimica, Ingegneria Chimica e Materiali, Università di L'Aquila, 67010 L'Aquila, Italy, Dipartimento di Chimica, Università di Roma "La Sapienza", P.le A. Moro 5, 00185 Roma, Italy, and Universidad de Santiago, Campus de Lugo, Facultad de Ciencias, Departamento de Quimica Fisica, 27002 Lugo, Spain

Received December 2, 1997. In Final Form: May 13, 1998

Sodium and rubidium deoxycholate (NaDC and RbDC, respectively) fibers have been drawn near the gelation point by lowering the pH of aqueous micellar solutions. Their X-ray diffraction patterns show a very close resemblance and can be interpreted by means of similar unit cell parameters and helical structures, formed by trimers arranged in 8/1 helices. Because the structures of the resulting fibers are connected with those observed in crystals, the helix of the RbDC crystal has been chosen to construct the 8/1 helix of the fibers. Calculations of interatomic distances support the 8/1 helix that can be used as a structural model of the NaDC micellar aggregates, especially near the gelation point. The lowering of pH within a narrow range in NaDC aqueous solutions causes a remarkable increase of the apparent hydrodynamic radius (R_h) and of the average scattered intensity. The intensity strongly changes within 2 °C around the temperature of the sol−gel transition. A bimodal R_h distribution, corresponding to very small and very big aggregates, is observed. The dominant mechanism causing the decay of the intensity autocorrelation function seems to be the translational motion of the center of mass of the aggregates. The absence of an appreciable rotational contribution is ascribed to the formation of roughly isotropic aggregates with spheroidal shape. It is proposed that the isotropic big aggregate is formed by helices randomly coordinated around a solvated hydrogen ion or a cluster containing hydrogen ions and water molecules, and that a network of cross-links, due to polar forces, connects the big aggregates and is responsible for the gel formation.

Introduction

Sodium and rubidium deoxycholate (NaDC and RbDC, respectively) form micellar aggregates. Their sizes depend on the ionic strength, pH, temperature, and concentration.[1] NaDC and RbDC give rise to the transitions: aqueous micellar solution (sol)−gel−fiber−crystal. The sol−gel transition occurs by varying, for example, ionic strength or pH. Glassy and birefringent fibers can be drawn from the gel and the aqueous micellar solution near the gelation point, and crystals can be obtained from the fibers by aging.[2−4] Because the X-ray diffraction patterns of these phases show correlated intensity distributions,[2−4] we thought we would have a good chance of finding similar structural units in the liquid and solid phases.[4,5] If this had been the case, the determination of the NaDC and RbDC crystal structures would have been sufficient to obtain an appropriate structural model of the micellar aggregates. Their unit cell constants and space groups are $a = b = 34.56$ Å, $c = 11.75$ Å, $\gamma = 120°$, $P6_5$ (NaDC), and $a = 19.83$ Å, $b = 19.31$ Å, $c = 11.59$ Å, $\gamma = 116.7°$, $P2_1$ (RbDC). The crystal structures are characterized (Figure 1) by helices around the 3_2 and 6_5 axes (NaDC) and 2_1 axis (RbDC). The structure of the RbDC crystals, obtained from the fiber by aging, has been solved.[6] Unfortunately, attempts to solve the NaDC crystal structure have been

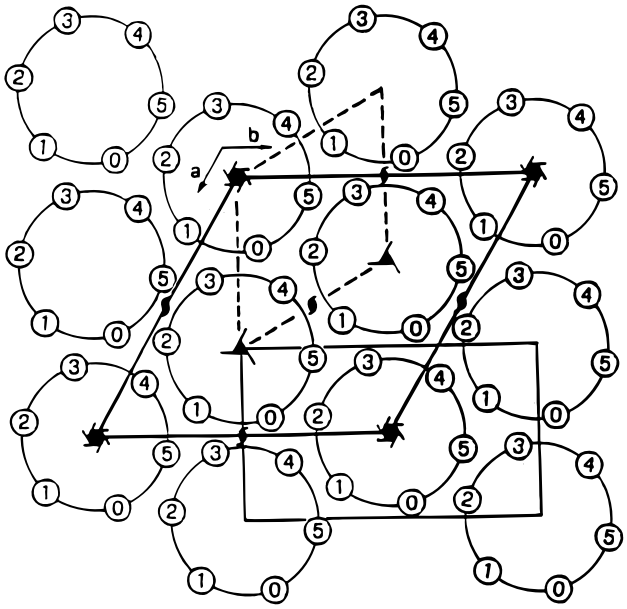

Figure 1. Schematic drawing of the *ab* hexagonal cell of the NaDC crystal viewed along *c* (thick full line). The small and large open circles represent deoxycholate anions and helices, respectively. The figures inside the small open circles indicate approximately their height on *c* in *c*/6 units. The broken lines show the approximate *ab* monoclinic cell of the RbDC crystal. The thin full lines represent the *ab* rectangular cell proposed for the NaDC and RbDC fibers.

* Author to whom correspondence should be addressed.
† Dipartimento di Chimica, Ingegneria Chimica e Materiali.
‡ Dipartimento di Chimica, Università di Roma "La Sapienza".
§ Universidad de Santiago.

(1) For leading references, see: Carey, M. C. In *Sterols and Bile Acids*; Danielsson, H., Sjøvall, J., Eds.; Elsevier/North-Holland Biomedical: Amsterdam, 1985; Chapter 13, p 345.
(2) Rich, A.; Blow, D. M. *Nature (London)* **1958**, *182*, 423.
(3) Blow, D. M.; Rich, A. *J. Am. Chem. Soc.* **1960**, *82*, 3566.
(4) Conte, G.; Di Blasi, R.; Giglio, E.; Parretta, A.; Pavel, N. V. *J. Phys. Chem.* **1984**, *88*, 5720.
(5) Campanelli, A. R.; Candeloro De Sanctis, S.; Giglio, E.; Pavel, N. V.; Quagliata, C. *J. Incl. Phenom. Mol. Recognit. Chem.* **1989**, *7*, 391.
(6) Campanelli, A. R.; Candeloro De Sanctis, S.; Giglio, E.; Petriconi, S. *Acta Crystallogr., Sect. C* **1984**, *C40*, 631.

S0743-7463(97)01312-7 CCC: $15.00
Published on Web 07/21/1998

unsuccessful because of a probable two-position disorder of the 3_2 helix around the 6_5 axis. However, some details of the NaDC crystal structure have been established, because the RbDC and NaDC crystal structures are strictly related (Figure 1) and very similar to each other.[4] The 3_2 and 2_1 helices have a pseudo-6-fold screw axis, a radius of ~10 Å, and six molecules in the identity period along the *c* axis. These left-handed helices are stabilized by ion−ion interactions between cations and carboxylate ions, ion−dipole interactions between cations and water molecules or hydroxyl groups, and a close net of hydrogen bonds (Figure 2). Surprisingly, the helices are mainly polar inside and apolar outside (notice, however, the hydroxyl group at C_3 in Figure 2). Apolar groups cover their outer lateral surface, which must be in contact with the aqueous medium in solution. Nevertheless, their solubility in water can be accounted for. In fact, the polar groups of the deoxycholate anions can be approached by water molecules that flow through the bases and the lateral surface of the helices, because the separation between two adjacent deoxycholate anions is sufficiently large.

Small-angle X-ray scattering (SAXS),[7] electron spin resonance (ESR),[7] extended X-ray absorption fine structure (EXAFS),[8−10] circular dichroism (CD),[11−13] nuclear magnetic resonance (NMR),[13−15] and quasi-elastic light-scattering (QELS)[16] techniques were used to study the NaDC and RbDC micellar aggregates and their interaction complexes with some probe molecules. The RbDC helix was assumed as an approximate model of the micellar aggregates in aqueous solutions, and resulted in agreement with the experimental data.

The structure of the micellar aggregates may undergo remarkable changes in the sol−gel−fiber transitions especially because of elongational stress. However, a better description of the micellar aggregates could arise from the knowledge of the NaDC and RbDC fiber structures because the fiber is a system more directly related to the aqueous micellar solutions than is the crystal, at least under conditions of high concentration and/or ionic strength and when the pH is ~7. Of course, the fiber model must be validated by means of solution measurements. An explanatory example is provided by the study of sodium and rubidium salts of glycodeoxycholic and taurodeoxycholic acids.[17,18] Their fibers were investigated by X-ray analysis. A 7/1 helix, constructed using as repetitive unit a trimer with a 3-fold rotation axis, was proposed as the structural unit of the fibers. This model was in satisfactory agreement with QELS[18] and electromotive force[18,19] measurements, which provided the distribution of micellar aggregation numbers for sodium taurodeoxycholate (NaTDC) aqueous solutions at different ionic strengths.

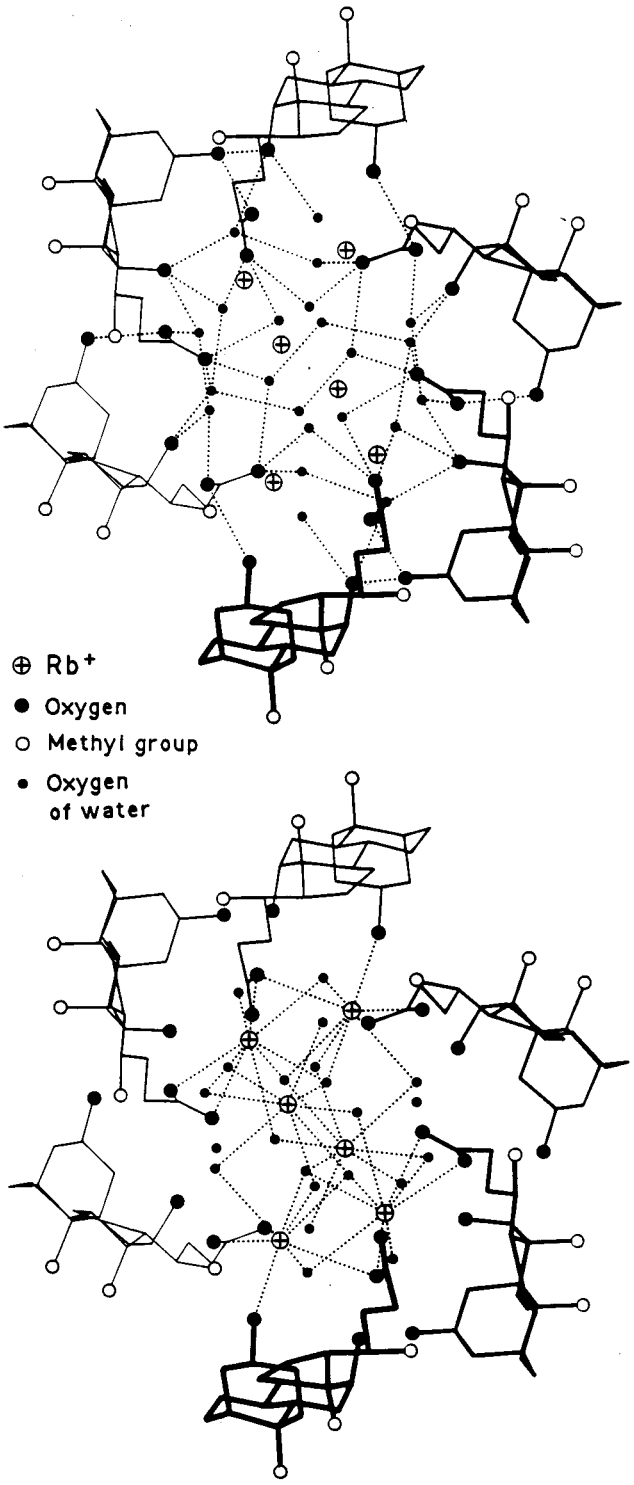

Figure 2. View of the clockwise helix in the RbDC crystal along the 2_1 helical axis. The broken lines represent hydrogen bonds (top) and ion−ion and ion−dipole interactions within 3.4 Å (bottom).

Hence, a model inferred from the NaDC fiber is probably more adequate than that observed in the crystal to represent the micellar aggregate structure because the fiber is drawn from an aqueous micellar solution near the gelation point. Reasonably, the same structural units of the solution are present with a certain degree of orientation in the fiber. The aim of this work is to acquire information

(7) Esposito, G.; Giglio, E.; Pavel, N. V.; Zanobi, A. *J. Phys. Chem.* **1987**, *91*, 356.
(8) Giglio, E.; Loreti, S.; Pavel, N. V. *J. Phys. Chem.* **1988**, *92*, 2858.
(9) Burattini, E.; D'Angelo, P.; Giglio, E.; Pavel, N. V. *J. Phys. Chem.* **1991**, *95*, 7880.
(10) D'Angelo, P.; Di Nola, A.; Giglio, E.; Mangoni, M.; Pavel, N. V. *J. Phys. Chem.* **1995**, *99*, 5471.
(11) Campanelli, A. R.; Candeloro De Sanctis, S.; Chiessi, E.; D'Alagni, M.; Giglio, E.; Scaramuzza, L. *J. Phys. Chem.* **1989**, *93*, 1536.
(12) D'Alagni, M.; Forcellese, M. L.; Giglio, E. *Colloid Polym. Sci.* **1985**, *263*, 160.
(13) D'Alagni, M.; Delfini, M.; Galantini, L.; Giglio, E. *J. Phys. Chem.* **1992**, *96*, 10520.
(14) Esposito, G.; Zanobi, A.; Giglio, E.; Pavel, N. V.; Campbell, I. D. *J. Phys. Chem.* **1987**, *91*, 83.
(15) Chiessi, E.; D'Alagni, M.; Esposito, G.; Giglio, E. *J. Inclusion Phenom. Mol. Recognit. Chem.* **1991**,*10*, 453.
(16) D'Alagni, M.; D'Archivio, A. A.; Galantini, L.; Giglio, E. *Langmuir* **1997**, *13*, 5811.
(17) D'Alagni, M.; D'Archivio, A. A.; Giglio, E.; Scaramuzza, L. *J. Phys. Chem.* **1994**, *98*, 343.
(18) Briganti, G.; D'Archivio, A. A.; Galantini, L.; Giglio, E. *Langmuir* **1996**, *12*, 1180.
(19) Bottari, E.; Festa, M. R. *Langmuir* **1996**, *12*, 1777.

Table 1. Observed (d_o) and Calculated (d_c) Spacings (Å) of Layer Lines for NaDC (c = 52.0 Å) and RbDC (c = 51.6 Å)

	NaDC		RbDC	
layer line	d_o	d_c	d_o	d_c
1	52.0	52.0	51.6	51.6
2			25.8	25.7
6	8.7	8.7		
7	7.4	7.4	7.4	7.4
8	6.5	6.5	6.5	6.5
9	5.8	5.8	5.7	5.7
15	3.5	3.5	3.4	3.4

on NaDC fibers and aqueous solutions that are near the gelation point by means of X-ray and QELS measurements, respectively.

Experimental Section

Materials. RbDC was obtained by adding to deoxycholic acid (Sigma) a little less than the equivalent amount of RbOH solution (Aldrich) and filtering the resulting suspension. NaDC (Calbiochem) and RbDC were twice crystallized from a mixture of water and acetone. No acetone was detected in the crystals by X-ray analysis and NMR spectra. NaDC/H_2O and RbDC/H_2O ratios of 4 and 10/3, respectively, were established by X-ray, density, and thermogravimetric measurements. Glassy and brittle fibers were drawn from viscous aqueous solutions of NaDC and RbDC obtained by adding HCl. Phosphate buffer (pro analysi) was purchased from Merck.

X-ray Measurements. Fibers of NaDC and RbDC were preferentially oriented microcrystalline specimens. Their X-ray diffraction photographs were recorded on flat and cylindrical films with Weissenberg, Debye−Scherrer, and Buerger precession cameras, using Cu Kα and Fe Kα radiations (λ = 1.5418 and 1.9373 Å, respectively). The density of NaDC (1.20 g cm^{-3}) and RbDC (1.26 g cm^{-3}) fibers was measured by flotation in a mixture of cyclohexane−carbon tetrachloride, the density of which was determined with an Anton Paar DMA 02C densimeter. Thermogravimetric analyses were accomplished with a Perkin-Elmer Model TGA7 apparatus equipped with a FT-IR Perkin-Elmer 1760X spectrometer. Melting points (566 and 614 K for NaDC and RbDC, respectively) were measured at atmospheric pressure with a Leitz 350 heating plate.

QELS Measurements. A Brookhaven instrument, with a BI-2030AT digital correlator with 136 channels and a BI-200SM goniometer, was used. The light source was an argon ion laser model 85 from Lexel Corporation operating at 514.5 nm. Dust was eliminated with a Brookhaven ultrafiltration unit (BIUU1) for flow-through cells, the volume of the flow cell being ∼1.0 cm^3. Nuclepore filters with a pore size of 0.1 μm were used. The samples were placed in the cell and were allowed to stand for 48 h prior to measurement to obtain reproducible data, while their temperature was kept constant within 0.5 °C by a circulating water bath. The scattered intensity and the time-dependent light scattering correlation function were analyzed at angles ranging from 30 to 150°. The scattering decays were analyzed by cumulant expansion up to second order, because higher order contributions did not improve the statistics. The apparent hydrodynamic radius was calculated by the Stokes−Einstein relationship.

Results and Discussion

X-ray Analysis of NaDC and RbDC Fibers. X-ray diffraction photographs typical of helical structures were taken of air-dried fibers of NaDC and RbDC. The most intense layer lines are clearly resolved into a series of spots. The NaCl and RbCl interplanar spacings were used to determine those of NaDC and RbDC. The spacings of the layer lines from 1 to 15 are practically equal for NaDC and RbDC and correspond to identity periods along the helical axis of 52.0 and 51.6 Å, respectively. The measured spacings of the most intense layer lines are shown in Table 1. All but one of the observed equatorial spacings listed

Table 2. Observed (d_o) and Calculated (d_c) Spacings (Å) and Miller Indices (h,k) of Equatorial Reflections for NaDC (a = 32.3, b = 18.7 Å) and RbDC (a = 34.1, b = 19.7 Å)

NaDC				RbDC		
d_o	d_c (h,k)			d_o	d_c (h,k)	
18.7	18.7 (0,1)			34.1	34.1 (1,0)	
16.1	16.2 (2,0)	(1,1)		25.8	25.8 (1,1)[a]	
12.2	12.2 (2,1)			19.7	19.7 (0,1)	
10.8	10.8 (3,0)			13.0	12.9 (2,1)	
9.3	9.3 (0,2)	(3,1)		9.9	9.9 (0,2)	(3,1)
9.0	9.0 (1,2)			9.5	9.5 (1,2)	
8.1	8.1 (4,0)	(2,2)		8.6	8.5 (4,0)	(2,2)
7.1	7.1 (3,2)			7.8	7.8 (4,1)	
6.1	6.1 (1,3)	(4,2)	(5,1)	6.1	6.1 (2,3)	
5.8	5.8 (2,3)			5.7	5.7 (6,0)	(3,3)

[a] This spacing belongs to a weak reflection that can be indexed as 110 by doubling the b axis.

Table 3. Comparison of Estimated Average Intensity (EAI) of the Layer Line (Index l) with Orders n of Bessel Functions for 8/1 and 7/1 Helices

l	EAI	n (8/1)	n (7/1)
0	strong	8, 0, −8	7, 0, −7
1	medium strong	1, −7	1, −6
2	weak	2, −6	2, −5
3	weak	3, −5	3, −4
4	very weak	4, −4	4, −3
5	weak	5, −3	5, −2
6	weak	6, −2	6, −1
7	strong	7, −1	7, 0, −7
8	strong	8, 0, −8	1, −6
9	medium strong	1, −7	2, −5
10	weak	2, −6	3, −4
11	very weak	3, −5	4, −3
12	very weak	4, −4	5, −2
13	very weak	5, −3	6, −1
14	weak	6, −2	7, 0, −7
15	medium weak	7, −1	1, −6
16	medium weak	8, 0, −8	2, −5
17	weak	1, −7	3, −4

in Table 2 can be indexed with the rectangular cell constants a = 32.3 Å, b = 18.7 Å (NaDC) and a = 34.1 Å, b = 19.7 Å (RbDC). One weak reflection of the RbDC fiber can be indexed as 1 1 0 by doubling the b axis. Because the ratio b/a is equal to tan 30°, the rectangular lattices can be derived from the hexagonal one of the NaDC crystal (Figure 1), where the shortest distance between two helices is 19.95 Å. The corresponding value of 18.7 Å observed in the NaDC fiber indicates that the helix of the fiber has a smaller cross section than that of the crystal. Each unit cell contains two helices with an identity period of ∼52 Å and with a radius of ∼9.3_5 Å (NaDC) and 9.8_5 Å (RbDC), assuming that the helices are represented by closely packed cylinders. The same estimated average intensity of the layer lines is observed for NaDC and RbDC (Table 3). A group of three intense layer lines near the meridian occurs at spacings of ∼7.4, 6.5, and 5.8−5.7 Å. The eighth layer line (spacing of 6.5 Å) is the most intense and, hence, its spacing could correspond to the helical axis projection of the distance between two consecutive equivalent points on the helix that presents eight (or nearly eight) points in the identity period. According to density or thermogravimetric measurements, the unit cells contain 48 steroid molecules (24 for each helix) and 3.2 or 3.6 (NaDC) and 3.9 or 3.9 (RbDC) water molecules for each steroid molecule, respectively. The resulting 8/1 helix has a trimer as a repetitive unit and can be generated by a rotation of 360°/8 = 45° and a translation of 6.5 Å. This helix is more elongated than that of the NaDC crystal because its average molecular projection on the helical

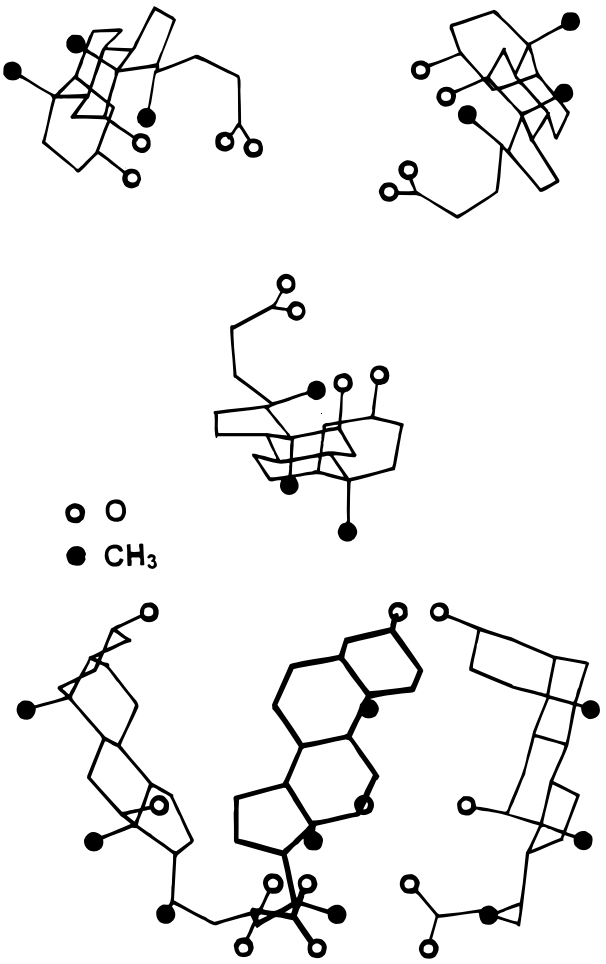

Figure 3. Projection of the anions of the trimer along the helical axis (top) and an axis perpendicular to the helical axis (bottom). The thicker line represents an anion nearer to the observer.

axis is 2.17 Å (1.96 Å in the crystal). The helical transform theory[20] supports the 8/1 helix, which presents appreciable intensity observed only for layer lines characterized by zero or near zero values of the permitted orders of Bessel functions (see Table 3 for a comparison with the 7/1 helix of NaTDC).

The structures of the 8/1 and 7/1 helices display some common characteristics. They have similar rectangular lattices, a nearly equal translation of the repetitive unit along the helical axis (6.4−6.5 Å), and similar repetitive units formed by trimers. Because the NaDC and RbDC crystals can be obtained from their fibers by aging, a possible model for the trimer of the 8/1 helix can be inferred from that observed in the RbDC crystal structure.[6] On the other hand, the trimer with a 3-fold rotation axis proposed for the 7/1 helix[18] is similar to that formed by three alternate anions of the RbDC helix at the same height on the helical axis (compare Figure 2 of this paper and Figure 3 of ref 18). Therefore, the trimer with a 3-fold rotation axis has been used as an approximate unit to construct the 8/1 helix, assuming the geometry of the anion observed in the sodium glycodeoxycholate crystal up to C_{24}.[11] Trimers with a 3_1 or 3_2 symmetry axis produce worse packings as in the case of the 7/1 helix and for the same reasons.[18]

The following sound arguments suggest that this model is valid also for the NaDC fiber and could adequately represent the structure of the NaDC micellar aggregates in aqueous solutions:

(1) The X-ray diffraction patterns of the NaDC and RbDC fibers show very similar intensity distribution, unit cells constants, and helical parameters.

(2) Attempts to solve the NaDC crystal structure with direct methods have shown that the two anions of the asymmetric unit around the 3_2 axis have atomic coordinates very similar to those of two anions of the RbDC crystal.

(3) The helix observed in the RbDC crystal was satisfactorily used to explain SAXS and ESR data collected for NaDC aqueous micellar solutions as a function of ionic strength, temperature, and NaDC concentration. The NaDC micellar aggregates resulted growing cylindrical objects in agreement with the helical model.[7]

(4) The study of interaction complexes in aqueous micellar solutions between NaDC or RbDC and probe molecules as bilirubin-IXα[11] and 2-bromopropane[9] by CD and EXAFS techniques showed that both the salts of the deoxycholic acid behave similarly. NMR and CD data confirmed that the probe molecules are micelle bound and located at the micelle−water interface. The most frequent binding site of the probe molecules was by far the C_{19} methyl group, which is the most protruding group from the helical axis of the RbDC helix in the crystal and in the fiber.[4,12−15]

Because the knowledge of a structural model is crucial for understanding some physicochemical properties, it was decided to better define the 8/1 helix. Calculations of interatomic distances were performed to get information on the arrangement of the anions in the trimer and to ascertain whether the resulting 8/1 helices suitably pack into the unit cell. The analysis was accomplished in the unit cell of the RbDC fiber. The hydrogen atoms were generated at the expected positions with a C−H bond length of 1.08 Å. Each anion of the trimer was moved as a rigid body by rotations and translations. The conformation of the side chain was changed by rotating around four bonds.[21] Suitable trimers were obtained, and each of them was used to generate the 8/1 helix by a clockwise rotation of 45° around and a translation of 6.5 Å along the helical axis (counterclockwise rotations give rise to short interatomic distances and, hence, the helix must be right-handed). The helix was considered reliable when the interatomic distances within the helix and among the helices of the unit cell were acceptable. The cations and the water molecules were omitted in the calculations, but inspection of the 8/1 helix shows that there is enough room for them. The 8/1 helix (Figure 3) presents an apolar lateral surface and is stabilized mainly by polar interactions as the 2_1 helix of the RbDC crystal. The helix at $a = b = 1/2$ gives rise to good contacts with the other helices. Good contacts are also found when the helix at $a = b = 1/2$ is very slightly rotated around and translated along the helical axis. It is interesting to note that negative changes in the volume, entropy, and enthalpy of micellization of NaDC aqueous solutions were inferred from pH and pNa measurements.[22] Moreover, hydrogen bonding was invoked as the driving force in the micellization process on the basis of viscosity, density, static ight scattering, conductivity, CD, NMR, pH, pNa, and solubilization of cholesterol measurements.[22−26] These

(20) Cochran, W.; Crick, F. H. C.; Vand, V. *Acta Crystallogr.* **1952**, *5*, 581.

(21) Giglio, E.; Quagliata, C. *Acta Crystallogr., Sect B* **1975**, *B31*, 581.

(22) Sugihara, G.; Tanaka, M. *Bull. Chem. Soc. Jpn.* **1976**, *49*, 3457.

(23) Sugihara, G.; Ueda, T.; Kaneshina, S.; Tanaka, M. *Bull. Chem. Soc. Jpn.* **1977**, *50*, 604.

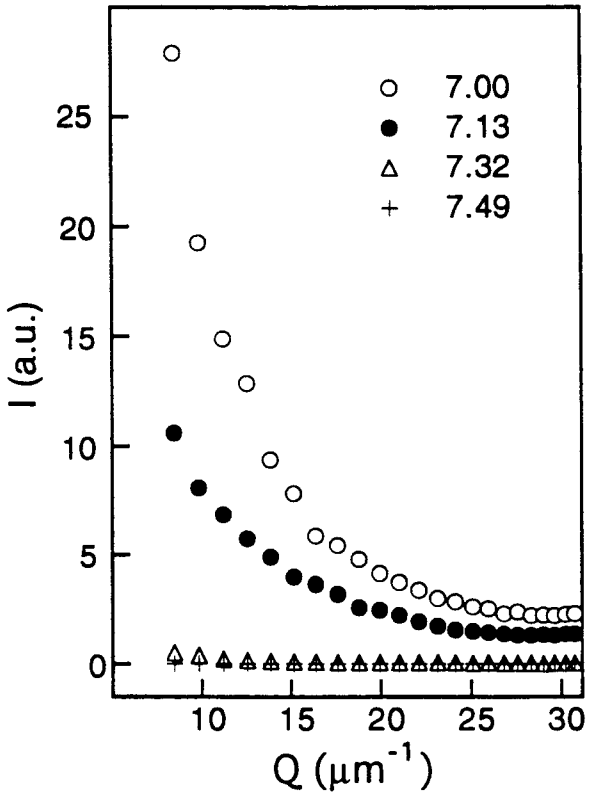

Figure 4. Average intensity scattered by a 49.3 mM NaDC aqueous solution at 40 °C as a function of the scattering vector *Q* at different pH values.

resultsindicate that polar interactions can be present in the micellar aggregates and agree with the model of the 8/1 helix.

A listing of the atomic coordinates of one anion of the trimer which forms a satisfactory 8/1 helix (Figure 3) is available as Supporting Information.

QELS Study of NaDC near the Gelation Point. Because the NaDC fibers were drawn from aqueous micellar solutions near the gelation point, the model inferred from the X-ray study of the fiber can be used to improve the understanding of the NaDC behavior in these solutions. Both temperature and pH strongly influence the formation of the gel, which is favored by the increase of the micellar size. The micellar size of NaDC aqueous solutions, acidified with HCl, dramatically increases within a narrow range of pH that depends on concentration and temperature. As an example, by fixing the NaDC concentration at 49.3 mM and the temperature at 40 °C, the values of the apparent hydrodynamic radius (R_h) are 397, 1098, and 1310 nm at pH 7.32, 7.13, and 7.00, respectively. The average intensity scattered by this sample at four pH values confirms the increase of the micellar size by decreasing the pH (Figure 4). Previous electromotive force measurements[27] showed an increasing uptake of hydrogen ions from the NaDC micellar aggregates when the pH is lowered and the solution tends toward the gel. This result explains the buffer capacity of NaDC solutions[3] and indicates that the big aggregates are protonated species.

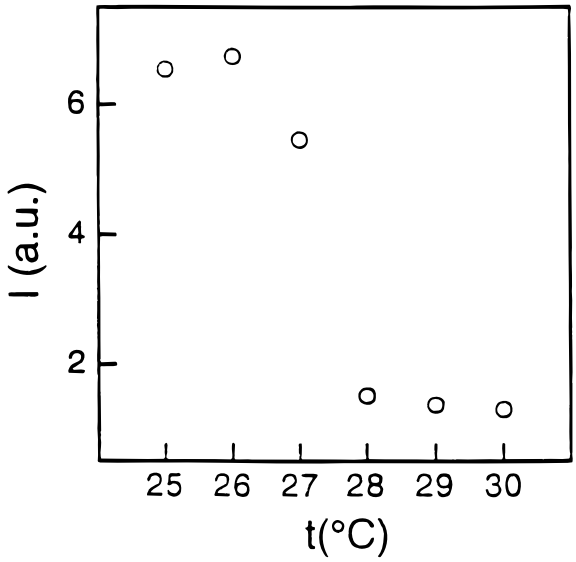

Figure 5. Average intensity scattered by a 49.3 mM NaDC aqueous solution (pH = 7.32) as a function of temperature near the sol−gel transition.

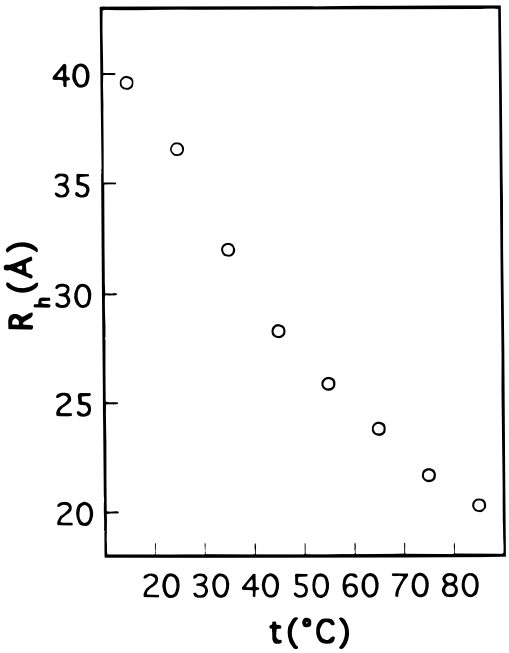

Figure 6. The R_h values of a 50 mM NaDC aqueous solution with 0.50 M NaCl (pH = 8.1) as a function of temperature. The average standard deviation is ±0.3 Å.

The effect of the temperature on the sol−gel transition is visible in Figure 5, where the sudden decrease of the average intensity scattered by a 49.3 mM NaDC aqueous solution at pH 7.32 is shown within the range 26−28 °C. A further increase of temperature from 35 to 55 °C does not change the average scattered intensity. A bimodal R_h distribution, corresponding to very small and very big aggregates with R_h values oscillating approximately around 1 and 400 nm, is also observed. A different behavior is found for a 50 mM NaDC aqueous solution with 0.50 M NaCl at higher pH. The plot of R_h as a function of temperature (Figure 6) shows that the increase of temperature in the range 15−85 °C causes a continuous decrease of R_h. Because association by hydrophobic interactions usually occurs in this range, the polar forces rather than the apolar ones could be the driving forces in the growth of the NaDC micellar aggregates, in accordance

(24) Sugihara, G.; Yamakawa, K.; Murata, Y.; Tanaka, M. *J. Phys. Chem.* **1982**, *86*, 2784.
(25) Murata, Y.; Sugihara, G.; Fukushima, K.; Tanaka, M.; Matsushita, K. *J. Phys. Chem.* **1982**, *86*, 4690.
(26) Murata, Y.; Sugihara, G.; Nishikido, N.; Tanaka, M. In *Solution Behavior of Surfactants: Theorethical and Applied Aspects*; Mittal, K. L., Fendler, E. J., Eds.; Plenum: New York, 1982; Vol. 1, pp 611−628.
(27) Bottari, E.; Festa, M. R.; Jasionowska, R. *J. Inclusion Phenom. Mol. Recognit. Chem.* **1989**,*7*, 443.

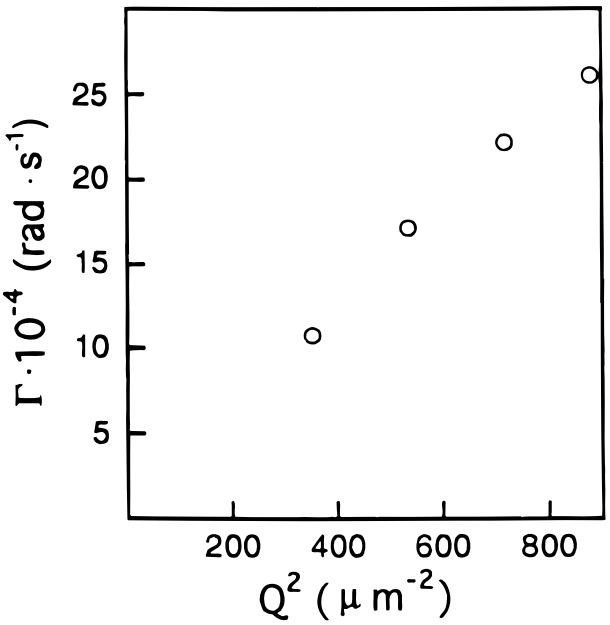

Figure 7. The values of Γ versus Q^2 for the small aggregates of a 49.3 mM NaDC aqueous solution at pH 7.32.

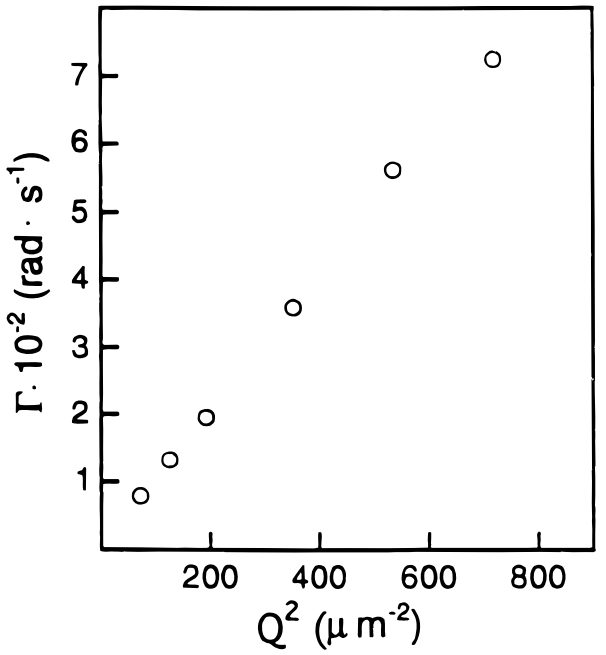

Figure 8. The values of Γ versus Q^2 for the big aggregates of a 49.3 mM NaDC aqueous solution at pH = 7.32.

with the helical model that is chiefly stabilized by polar forces. Thus, the approximately constant intensity and R_h values show that the big aggregate is not appreciably affected by the temperature within the range 35−55 °C and, therefore, is characterized by structure and forces that are different from those of the helical model.

To determine the dominant mechanism causing the decay of the intensity autocorrelation function, its first cumulant (Γ) is plotted as a function of Q^2 (Q is the scattering vector). Linear fits in Q^2 with an intercept near the origin characterize the small (Figure 7) and the big (Figure 8) aggregates, and point out that the dominating relaxation process is the translational motion of the center of mass of the aggregates. This result is expected in the case of small aggregates in the regime where $QR \leq 1$ (R is the radius of gyration), because at low wavevector values, the small aggregate scatters as a point and, therefore, the orientation of the aggregate is irrelevant. In the case of big aggregates, the measurements are performed in the regime where $QR \geq 1$ and the decay should be influenced by rotational diffusion.[28] The absence of this contribution could be ascribed to the formation of roughly isotropic aggregates with spheroidal shape. Because their formation depends on the decrease of pH, a possible model of the big aggregate is a set of helices, having their helical axes randomly oriented, which irradiate through a spherical surface from a center formed by a solvated hydrogen ion or a cluster containing hydrogen ions and water molecules. Previously, the effect of alkali cations on the sol−gel transition temperature of deoxycholic acid in aqueous solutions was studied by conductivity measurements.[29] This temperature, together with the stability of the aggregates, increases with the decreasing of the cation crystallographic radius. Of course, a shorter crystallographic radius implies shorter distances of the cation with the carboxylate groups and stronger polar interactions. In this connection it is interesting to note that the addition of calcium ions to aqueous solutions of sodium glycodeoxycholate causes the formation of large micellar aggregates. QELS data seem to indicate that sodium glycodeoxycholate micellar aggregates are held together by calcium ions. The bile salt anions have a greater affinity for the calcium than for the sodium ion because, although the distances of these ions with the oxygen atoms of carboxylate groups are nearly equal, the calcium ion has a higher charge and charge density.[30] As an example, the calcium ion is coordinated to four carboxylate groups in a crystal structure of calcium glycodeoxycholate.[30] Therefore, it is reasonable to hypothesize that the hydrogen ions, which could form very short distances and very strong interactions with the oxygen atoms of carboxylate groups, act as aggregation centers of the NaDC helices, thus forming the big aggregates.

A further indication on the nature of the NaDC gel can be inferred from a study of the sol−gel transition accomplished by conductivity measurements as a function of pressure and temperature. The gel formation, obtained by adding HCl, is accompanied by negative changes of volume, entropy, and enthalpy.[23] Because the sol−gel transition is reversible, the gel is produced by polar and apolar interactions rather than by covalent bonds. Generally the polar interactions (i.e., ion−ion, ion−dipole, and, especially, hydrogen bonding) lead to negative changes of volume and enthalpy, whereas the apolar ones (i.e., hydrophobic interactions) cause positive changes of volume and entropy. Thus, the gel could be characterized by a network of cross-links due to polar forces that connects the big aggregates and gives rise to a remarkable increase of the average scattered intensity (Figure 5). Previously, it was pointed out that NaDC in aqueous solutions gives rise to four concentration regions in which are present monomers, oligomers, polymer-like (helical) aggregates, and nearly spherical aggregates.[26] On the whole, our findings agree fairly well with this picture.

Acknowledgment. This work was sponsored by the Italian Ministero per l'Università e per la Ricerca Scientifica e Tecnologica (Cofin. MURST 97 CFSIB). A. J. thanks the Xunta de Galicia for financial support.

LA971312R

(28) Klein, R.; Weitz, D. A.; Lin, M. Y.; Lindsay, H. M.; Ball, R. C.; Meakin, P. *Prog. Colloid Polym. Sci.* **1990**, *81*, 161.
(29) Botré, C.; Cicconetti, P. A.; Lionetti, G.; Marchetti, M. *J. Pharm. Sci.* **1967**, *56*, 1035.
(30) D'Archivio, A. A.; Galantini, L.; Gavuzzo, E.; Giglio, E.; Mazza, F. *Langmuir* **1997**, *13*, 3090.